PCCP

Accepted Manuscript

This is an *Accepted Manuscript*, which has been through the Royal Society of Chemistry peer review process and has been accepted for publication.

Accepted Manuscripts are published online shortly after acceptance, before technical editing, formatting and proof reading. Using this free service, authors can make their results available to the community, in citable form, before we publish the edited article. We will replace this *Accepted Manuscript* with the edited and formatted *Advance Article* as soon as it is available.

You can find more information about *Accepted Manuscripts* in the Information for Authors.

Please note that technical editing may introduce minor changes to the text and/or graphics, which may alter content. The journal's standard Terms & Conditions and the Ethical guidelines still apply. In no event shall the Royal Society of Chemistry be held responsible for any errors or omissions in this *Accepted Manuscript* or any consequences arising from the use of any information it contains.

ROYAL SOCIETY OF CHEMISTRY

www.rsc.org/pccp

Physical Chemistry Chemical Physics RSCPublishing

ARTICLE

LEIS and XPS investigation into the growth of cerium and cerium dioxide on Cu(111)

Cite this: DOI:

G. Vári,[a] L. Óvári,[b,*] J. Kiss,[b] and Z. Kónya[a,b]

Received
Accepted

DOI:

www.rsc.org/

The controlled growth of Ce and CeO_2 was investigated on Cu(111) applying low energy ion scattering spectroscopy (LEIS) and X-ray photoelectron spectroscopy (XPS). Previous LEIS studies on metallic and oxidised cerium deposits using other metallic substrates reported serious difficulties related to the neutralization of noble gas ions. For this reason, a special attention was paid here to reveal possible matrix effects for the neutralization ("neutralization effects"), which would severely hinder quantitative evaluation of the LEIS data. The adsorption of O_2 on Cu(111) induced no neutralization effects either with He^+ or Ne^+. Similarly, no neutralization effects were identified using He^+ upon the deposition of metallic Ce on Cu(111), but it arises for the Ce peak monitored with Ne^+. The initial growth of Ce is two dimensional up to Θ_{Ce}~0.5 ML, while almost complete coverage of Cu(111) is achieved at Θ_{Ce}=2 ML. CeO_2(111) was deposited evaporating Ce in a background of O_2 at a sample temperature of 523 K. No neutralization effects were observed either with He^+ or Ne^+. In harmony with literature data, the growth mode is three dimensional. Here it was demonstrated that the continuity of the film, which could be efficiently checked by LEIS, is influenced by the applied oxygen pressure in the range of 5×10^{-7} - 3×10^{-6} mbar. At $p_{O2}=3\times10^{-6}$ mbar the film was not completely closed even at relatively large coverages (16 ML), and a significant part of copper atoms were oxidized to Cu^{1+}. Deposition of CeO_2 at $p_{O2}=5\times10^{-7}$ mbar was characterized by a nearly perfect wetting, with metallic copper atoms at the interface, and with slightly more reduced ceria layer.

Introduction

Cerium dioxide (CeO_2) is an efficient support or promoter in many catalytic reactions, such as automotive exhaust catalysis, water gas shift reaction (WGS), steam reforming of ethanol (SRE), catalytic removal of SO_x, electrochemical oxidation of hydrocarbons, *etc*.[1-7] Most importantly, since it is easily reducible to Ce_2O_3, it can act as an oxygen buffer. Apart from this aspect, its basic character can also have a role in catalytic transformations.

For a deeper understanding of surface processes during complicated catalytic reactions, it is useful to construct simplified, but well controlled experimental model systems, using oxide single crystals or single crystalline oxide films, and preparing nanoclusters of the active metal on top.[8-13] The low conductivity of CeO_2 single crystals (e.g. compared to that of TiO_2) motivated an intense research aiming at the preparation of ultrathin single crystalline films of CeO_2 using various metallic supports, such as Ru(0001),[14,15] Cu(111),[16-23] Pd(111)[24] *etc*.

Since the interaction of oxygen and the support metal single crystal is an important characteristic of these systems, it is useful to briefly summarize here the related previous results, focussing on Cu(111), the substrate used in the present study. The adsorption of O_2 on Cu(111) was thoroughly investigated in the pressure range of ~1×10^{-6} mbar at both 300 K and elevated temperatures.[23,25-29] It was demonstrated by STM that oxygen is capable of abstracting Cu from the terraces at room temperature, starting from the step edges and vacancy sites.[29] A surface oxide forms at 300 K with a structure close to Cu_2O(111), though containing many defects.[29] Extended areas of the so called "44" structure ($\sqrt{73}R5.8° \times \sqrt{21}R-10.9°$) can be produced performing the oxidation at higher temperatures (423-600 K).[23,29] This structure originates from a distorted Cu_2O(111)-like layer grown epitaxially on the Cu(111) substrate. The Cu_2O(111)-like "44" layer possesses the same honeycomb structure as the Cu_2O(111) surface, but with the coordinatively under-saturated Cu atoms (cus-Cu) removed.[23,27-30] Annealing the "44" structure in UHV at 573-673 K led to the transformation of the surface to the "29" structure.[29] The formation of the "29" structure ($\sqrt{13}R46.1° \times 7R21.8°$) was also reported after oxidation (~7×10^{-7} mbar O_2) at 700-750 K.[23] In the "29" surface oxide the hexagonal structure associated with Cu_2O(111) is more distorted; it contains 0.52 ML (monolayer) of O. Further

Physical Chemistry Chemical Physics Accepted Manuscript

oxidation of Cu(111) is not possible at $p<10^{-5}$ mbar (up to ~2000 L, 1 L=10^{-6} Torr × 1 s).[27,28]

CeO_2(111) layers were previously prepared either depositing Ce in O_2 atmosphere ($2 \times 10^{-7} - 1 \times 10^{-6}$ mbar) or evaporating Ce in ultrahigh vacuum (UHV), followed by an oxidation step. The deposition temperature also varied (100-723 K, in some cases applying heating ramps during deposition), but a high temperature treatment (at T≥520 K in ~5×10^{-7} mbar O_2) was always required to obtain a well ordered film.[16-23] There is general agreement that the CeO_2(111)/Cu(111) system thermodynamically follows the Volmer-Weber (3D) growth mode, probably due to the weak interaction between the oxide and the support.[19,20] Investigation of the initial growth of CeO_2(111) on Cu(111) revealed that the dissociation of O_2 is facilitated by the presence of CeO_2 nanoparticles, and there is a spill-over of oxygen to the copper.[23] While in some cases the presence of extra spots in the LEED structure or the observed periodicities in (overlapping) moiré patterns led some authors to hypothesize oxygen induced reconstructions of the interfacial copper layer,[19,23] in other cases it was assumed that the CeO_2(111) layer replaces surface copper oxides.[20] The most frequently applied recipe for the preparation of continuous CeO_2(111) layers consists of the deposition of Ce in an O_2 background of ~5×10^{-7} mbar at 523 K at a rate of 0.08-0.15 ML/min. 1 ML of CeO_2(111) layer is defined as one O-Ce-O trilayer of the fluorite structure of bulk CeO_2 (3.13 Å). This method yields a well oriented, but corrugated film with relatively small terraces (10 nm).[20,21] There is a slight scatter in the literature regarding the minimum coverage required to obtain a continuous film with this recipe. While in Ref [18] the 2.5 ML thick film was found to be continuous, based on the complete disappearance of the Cu(111) LEED pattern, in other cases[19] even at 5 ML the film was still slightly incomplete (LEED, STM). Traces of Cu (~0.002 ML) on the outermost atomic layer were detected even for ~10 ML of CeO_2.[31] For model catalytic studies, the continuity of the film is important to avoid direct contact of reactants with the metal single crystal substrate. In the present study low energy ion scattering (LEIS) was used to monitor in situ the tightness of the ceria film. Since this method provides information almost exclusively about the outermost atomic layer, when performed with noble gas ions,[32] it is particularly suited for this purpose.

Although the adsorption of metallic Ce on Cu(111) is also important for a complete understanding of the preparation of ceria nanolayers on Cu(111), related literature data is rather scarce. The deposition of Ce metal on a Cu film at 300K led to significant intermixing of Ce and Cu.[33] The bulk solubility of Ce in Cu and Cu in Ce is very limited, below 0.4 at.% in our temperature range (T≤900 K), but several copper-cerium intermetallic compounds exist: Cu_6Ce, Cu_5Ce, Cu_4Ce, Cu_2Ce, and CuCe.[34] The loss of material (CeO_2 average thickness) observed during repeated annealing of CeO_2(111) films on Cu(111) up to 823 K was attributed to the diffusion Ce into the bulk.[19]

Since no systematic LEIS study appeared so far about the deposition of Ce and CeO_2 on Cu(111), it seemed to us worthwhile to investigate this system in detail, completed by X-ray photoelectron spectroscopy (XPS). The intensity of an ion scattering peak depends sensitively on the neutralization probability for the impinging noble gas ions upon the collision with the surface atoms.[32] Although matrix effects for the neutralization probability (*i.e.* changes in the neutralization during scattering on the given atom as a function of its chemical environment), sometimes simply referred to as "neutralization effects", are relatively rare in LEIS, these can severely hinder a quantitative evaluation of the data, if they arise.[32] For this reason a special attention was paid in this study on neutralization effects. Note that previous LEIS studies, devoted to the deposition of Ce on other metal surfaces reported serious difficulties. The Ce LEIS peak was not detectable at all with He^+ on Rh(111) and it was very weak with Ne^+. Moreover, significant changes in the neutralization probabilities were observed with both projectiles.[35] After the deposition (and oxidation) of Ce on Pd(111) at room temperature, the Pd LEIS peak decreased rapidly, but no Ce peak could be observed by LEIS using He ions, attributed mostly to the large neutralization probability of He^+, possibly due to quasi resonant neutralization.[24] However, with Ne^+ the Ce peak was easily detectable. A slight attenuation of the neutralization probability of Ne^+ (on Ce) was observed due to O_2 adsorption.

Experimental

The experiments were carried out in a UHV chamber with a base pressure of 5×10^{-10} mbar. It was equipped with a Leybold hemispherical analyser for performing LEIS, XPS, and Auger electron spectroscopy (AES) measurements. For LEIS a constant retardation ratio was applied, while XPS was performed with a constant pass energy. A quadrupole mass spectrometer (QMS) was used in this work for rest gas analysis. A SPECS IQE 12/38 ion source was used for LEIS. He^+ or Ne^+ ions with 800 eV kinetic energy were applied at a low ion flux, ~0.03 μA/cm^2. The incident and detection angles were 50° (with respect to the surface normal), while the scattering angle was 95°. The angle between the "incident plane" (the plane defined by the ion source axis and the surface normal) and the "detection plane" (the plane defined by the surface normal and the analyzer axis) was 53°. An Al Kα X-ray source was applied for XPS. The binding energy scale was calibrated against the $4f_{7/2}$ peak of a thick Au layer (84.0 eV) and the $2p_{3/2}$ peak of the clean Cu(111) surface (932.6 eV). The detection angle was 16° off normal. Peak fitting of the Ce 3d XPS region and of the LEIS spectra obtained with helium was executed with the help of XPSPEAK 4.1 using Gauss-Lorentzian sum line shapes and Shirley baselines.[36] For LEIS and in some cases for the Ce 3d XPS region asymmetry was also allowed applying an exponential tailing function.

The Cu(111) single crystal was a product of MaTeck (purity: 99,9999%, orientation accuracy: 0.1°). Its temperature was measured by a chromel–alumel (K-type) thermocouple inserted into a hole in the crystal. It was heated radiatively with a W filament placed behind the crystal. The surface was routinely

Physical Chemistry Chemical Physics Accepted Manuscript

 This journal is © The Royal Society of Chemistry 2012

cleaned applying cycles of Ar^+ ion sputtering (10 μA/cm^2, 1.5 keV) at 300 K and vacuum annealing (5 min, 1000 K).
The purity of O_2 (Linde) was 99.995 %. One monolayer of O is defined as the surface concentration of Cu(111) (1.78×10^{15} atoms/cm^2). Ce (99.9%) was deposited by a commercial 4-pocket PVD source (Oxford Applied Research) using a Ta crucible. One monolayer of CeO_2 is defined as a complete CeO_2(111) trilayer (i.e., O-Ce-O stack, 7.87×10^{14} Ce atoms/cm^2) having a thickness of 3.13 Å.[37] The phase diagram of metallic Ce contains three phases at moderate conditions (T<1000 K, p<3 GPa): α (fcc), β (dhcp), and γ (fcc).[38] For metallic Ce, here we define the one ML coverage as the surface concentration of the close packed (0001) surface of the dhcp bulk β phase, because it is the thermodynamically stable phase at room temperature. In this way 1 ML of Ce ~ 8.53×10^{14}cm^{-2}.[37] Although in terms of Ce surface concentration there is a small difference in the coverage scale for Ce and CeO_2, we choose these definitions, because in case of layer-by-layer growth complete coverage of the Cu(111) surface is achieved at 1 ML in both cases. The coverage of Ce was checked by a quartz crystal microbalance (QCM), and the evaporation rate was 0.07 ML/min for both Ce and CeO_2.

Results and discussion

Since in previous LEIS studies on the adsorption of Ce on Rh(111) and Pd(111) neutralization effects arose,[24,35] this issue was carefully checked in the present work. The charge transfer between surface atoms and the noble gas projectile can proceed according to different mechanisms.[32] Resonant neutralization (RN) occurs, when an electron from the highest lying (partly) filled valence (conduction) band of the target tunnels into an empty excited level of the projectile. If a deeper filled band of the solid is aligned with the 1s level of the projectile, then a resonant electron transfer can proceed in a similar way. Since this alignment is generally not perfect, this process is called quasi resonant neutralization (qRN). Electrons from the high lying conduction/valence band of the solid can be transferred to the 1s level of the projectile, if the energy released in this step is transferred to an Auger electron from the target. This Auger neutralization (AN) mechanism is operative in every case, though resonant processes typically dominate, if they arise. If the primary ion energy exceeds a threshold, and consequently the minimum distance between the surface nucleus and the ion is small enough then new neutralization channels open (collision induced neutralization, CIN). Reionization processes can play a significant role as well, influencing both the background of the spectrum and the single scattering peak.[32]
If there are no neutralization matrix effects for the system consisting of element A and B, then the observed intensity for A (I_A) is a linear function of that of B (I_B), when the surface composition is varied, if the geometrical shadowing effect of a deposited atom does not change with coverage. The control of this behaviour is a widely used check for the occurrence of neutralization effects.[32,39] This method was applied also in the present study.

The adsorption of O_2 on Cu(111)

Although the adsorption of O_2 on Cu(111) was previously investigated in detail, as summarized in the Introduction, it seemed to us necessary to perform some measurements on the O/Cu(111) system focussing on possible neutralization effects. It serves mostly for comparison with the CeO_2/Cu(111) surface. O_2 was dosed for 5 min on the Cu(111) surface at 300 K, at pressures increased stepwise. Surface oxygen was not removed in between the adsorption steps. LEIS spectra, obtained in this measurement with He, are displayed in Fig. 1 (a). The peak areas (using He and Ne) and the pressure applied for the last adsorption step are shown in Fig. 1 (b) as a function of the *cumulative* O_2 exposure, measured in L (1 L = 10^{-6} Torr s, 1 Torr=1.33 mbar).
The small peak observed at ~507 eV is not due to surface contamination (the cleanliness of the Cu(111) surface was controlled also by XPS and AES), but can be assigned to an instrumental artifact: the ion source produced a small quantity of He^+ ions with a kinetic energy of eU_f, where U_f is the potential of the focussing electrode. These ions were also scattered on the surface Cu atoms, resulting in a distinct peak at a position, which scaled appropriately with the focus voltage, while keeping the primary energy on the ion supply constant. The intensity of this "ghost" peak was ~0.4 % of that of the main peak. This contribution was removed via peak fitting during the quantitative evaluation of the O peak.
In parallel with the enhancement of the O LEIS area obtained with He (denoted O (He)) due to the accumulation of O on the surface, the copper peaks obtained with helium (Cu (He)) and neon (Cu (Ne)) decreased. This process reached a saturation at ~400 L (Fig. 1(b)), in accordance with a previous LEIS study on O_2/Cu(111).[40] Since in Ref. [40] the occurrence of neutralization effects was not addressed in detail, the linearity of the Cu – O curve was analysed here. As displayed in Fig. 1(c), the Cu (He) area decreased linearly with the increase of the O (He) signal. This implies that the O coverage is proportional to the O (He) LEIS signal, and each adsorbed oxygen atom attenuates the Cu (He) signal on average to the same extent, allowing the quantitative evaluation of the data. The above statement holds for the shadowing of the copper surface by oxygen also using neon, since the Cu (Ne) *vs.* O (He) curve was also linear (Fig. 1(c)). Consequently, the Cu (Ne) *vs.* Cu (He) curve, corresponding to the O_2 adsorption experiment, was also linear (Fig. 1(d)). However, this latter straight line does not pass through the origin, or in other words, the adsorption of oxygen attenuates the Cu (He) peak more steeply than the Cu (Ne) peak. The shielding effect of oxygen is stronger, when helium is used. Since LEIS spectra with He^+ were recorded before spectra with Ne^+, one might argue that this effect is an artifact, and the intercept of the linear in Fig. 1(d) with the vertical axis is influenced by the sputtering effect of Ne^+ ions. However, this is not the case, since the repetition of the experiment with 5 times higher Ne^+ flux gave qualitatively similar results and the slope in Fig. 1(d) was attenuated only by 14%.

Physical Chemistry Chemical Physics Accepted Manuscript

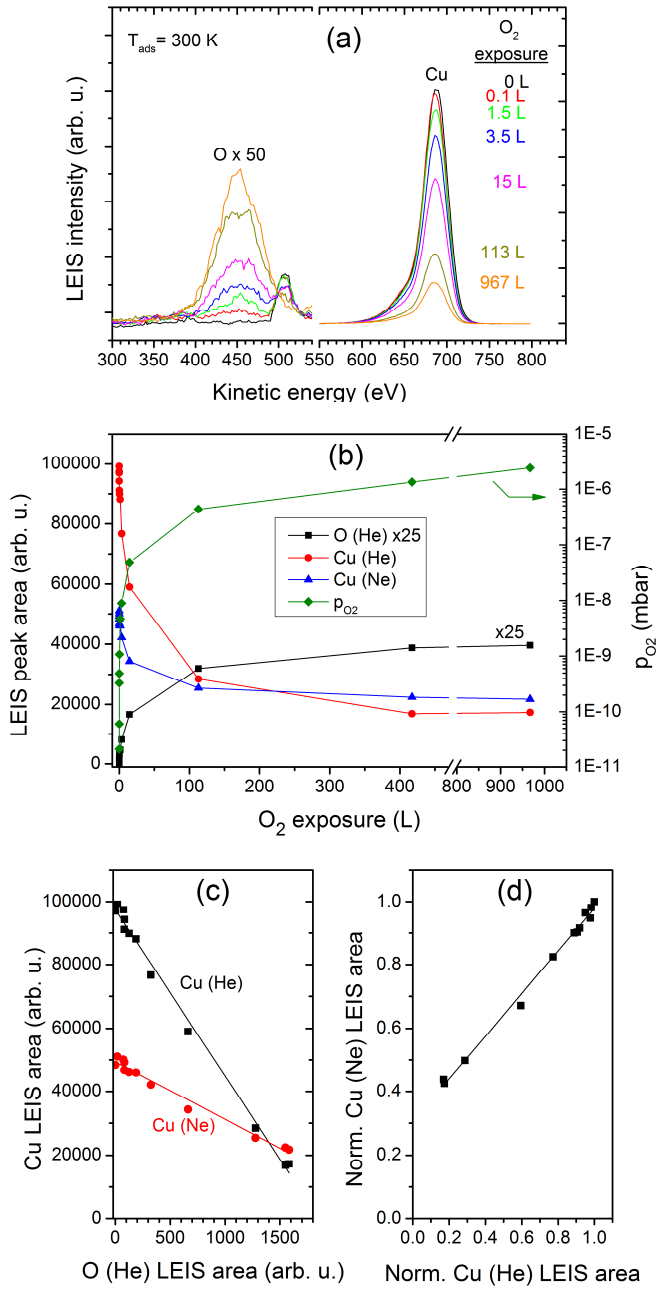

Fig. 1. (a): LEIS spectra obtained after exposing the Cu(111) surface at 300 K to O_2 at stepwise increased pressures for 5 min each. The surface oxygen was not removed in between the adsorption steps. The cumulative O_2 exposure is shown beside each spectrum. (b): LEIS peak areas (of O and Cu using He, and of Cu using Ne) obtained in the measurement described for (a). For each O_2 adsorption step the applied pressure is also shown as a function of the cumulative oxygen exposure (vertical scale on the right). (c): Copper LEIS peak areas obtained with He and Ne in the measurement described for (a) displayed as a function of the O LEIS peak area obtained with He. (d): The Cu peak area obtained with Ne as a function of the Cu area detected with He.

For the understanding of the differences in the shielding effect of oxygen with helium and neon, it is worth to consider that during the scattering of He^+ ions on adsorbed O atoms a so called shadow cone is formed behind the O nuclei, where the projectile cannot penetrate.[32] It is not the case for Ne ions, which are heavier than O, and can reach Cu atoms behind O. Nevertheless, copper atoms are partly shadowed by oxygen also using neon for two reasons: (i) there is a deviation of Ne^+ ions by O anyhow; (ii) only those neon trajectories contribute to the Cu peak, which correspond to single scattering events, *i. e.* when there is no significant impact with oxygen. For double and multiple scattering the neutralization is generally too efficient for that event to be observed, and in case it is detectable, the peak energy is different from the single scattering peak.[32] Note that it was previously demonstrated that neutralization does not solely happen in the close vicinity of the target surface atom, but also when the noble gas ion travels by neighbouring atoms (trajectory dependent neutralization), modifying also the intensity of the single scattering peak, such as for O/Ni(100), O/Cu(100) and Pb(111).[41-43] This process can operate to a different extent for He and Ne. Although this phenomenon, strictly speaking, is a neutralization effect, it does not necessarily impede a quantitative analysis. It was suggested that a shell-like neutralization region is operative around neighbouring nuclei,[43] which in a certain sense can be considered a modification of the size of the shadow cone of neighbour atoms. Although we cannot exclude a similar effect in our case, the linear behaviour presented in Fig. 1 (c) proves that quantitative information can be extracted from our data. Due to the differences in the scattering of He^+ and Ne^+ on O/Cu(111) mentioned above, it is not expected that the diminution of the Cu LEIS peak induced by the same amount of adsorbed O is identical for the two noble gases.

The linear dependence of the Cu (He) area on the O (He) area can be written as

$$A_{Cu} = A_{Cu}(0) - A_O/S_O, \qquad (1)$$

where A_{Cu} and A_O are the Cu (He) and O (He) areas, while $A_{Cu}(0)$ is the Cu (He) area of the clean copper surface. This can be transformed to

$$\zeta_{Cu} + \zeta_O = 1, \qquad (2)$$

where $\zeta_{Cu}=A_{Cu}/A_{Cu}(0)$, and $\zeta_O=A_O/(A_{Cu}(0)\times S_O)$ are the fractions of the surface covered by Cu and O, respectively. S_O is the relative sensitivity factor for O, which can be obtained as the reciprocal slope of the Cu (He) *vs.* O (He) curve. S_O=0.0191 under our circumstances.

The saturation O coverage was estimated also from the O 1s and Cu 2p XPS areas obtained after exposing the Cu(111) surface to 3×10^{-6} mbar O_2 for 5 min at 300 K (680 L). The application of standard inelastic-mean-free-path (imfp) and photoelectric cross section values yielded Θ_O = 0.76 ±0.1 ML.[44,45] Since saturation with O attenuated the Cu (He) LEIS peak by 83%, it can be concluded that one surface O atom shadows approximately one Cu atom in ion scattering experiments performed with He, at our experimental conditions.

Physical Chemistry Chemical Physics Accepted Manuscript

This journal is © The Royal Society of Chemistry 2012

The growth of Ce on Cu(111)

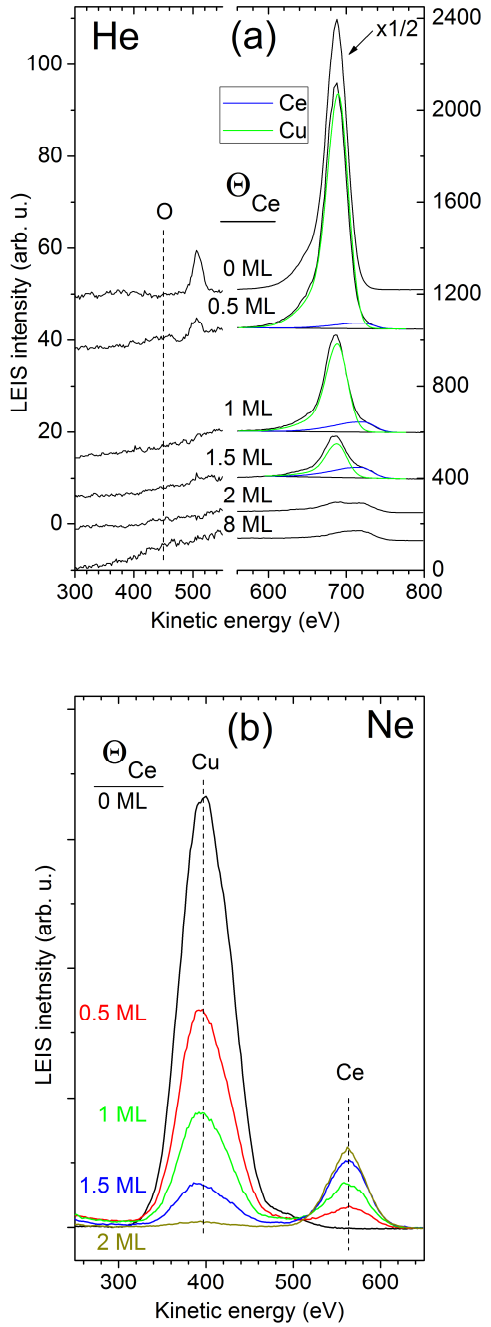

Fig. 2. LEIS spectra obtained with He (a) and Ne (b) after depositing Ce on the Cu(111) surface at 300 K. Each dose of Ce was evaporated on a clean Cu surface. Note that the vertical scale for the low kinetic energy part of (a) is 20 times more sensitive than the scale for the higher kinetic energy part. In addition, the Cu peak of the clean Cu(111) surface (0 ML) in (a) is reduced by a factor of 2.

As a next step, the growth of Ce was investigated on Cu(111) at 300 K. In Fig. 2 LEIS spectra obtained with He and Ne are shown after depositing Ce on the Cu(111) surface at 300 K. Each dose of Ce was evaporated on the clean Cu surface. The same ghost Cu peak was observed at ~507 eV as mentioned above about the oxygen adsorption measurements. Importantly, in spite of the well-known reactivity of metallic cerium, the O (He) peak was very small, undetectable on the majority of spectra (Fig. 2(a)), indicating the almost complete lack of oxygen containing contaminants (CO, H_2O) during these measurements. Since the Cu (He) peak overlaps the Ce (He) component, peak fitting was performed. The peak areas obtained with He and Ne as a function of Ce coverage are shown in Fig. 3 (a) and (b), respectively.

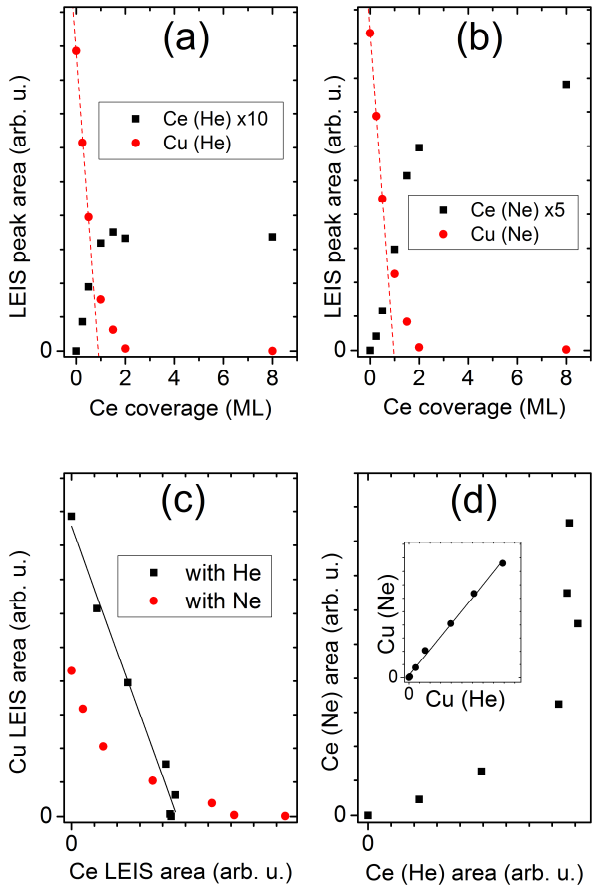

Fig. 3. The change of Ce and Cu LEIS peak area obtained with He (a) and Ne (b) during the deposition of Ce on Cu(111) at 300 K. Linear fits on the first three Cu areas (up to a cerium coverage of 0.5 ML) are presented as dashed lines for both (a) and (b). In (c) the Cu LEIS area is shown as a function of the Ce area with both He and Ne. For the data points obtained with He a linear fit is also displayed. In (d) the Ce (Ne) area obtained in the same experiment is plotted against the Ce (He) area, while in the inset the Cu (Ne) area is shown as a function of the Cu (He) area. For the latter a linear fit is also presented.

The observed Ce (He) peak was rather small even at Θ_{Ce}=8 ML, when the Cu (He) peak was completely suppressed by the cerium overlayer. This fact indicates that LEIS with He is much more sensitive to Cu than to Ce. At our experimental conditions the difference is a factor of 24. This observation is in line with previous studies reporting the inability in detecting the Ce LEIS peak with He, owing probably to the high neutralization probability.[24,35] Due to the fact that our scattering angle is relatively small (95°), resulting in higher signal to noise ratios, the Ce peak was well detectable.

Physical Chemistry Chemical Physics Accepted Manuscript

In order to check if neutralization effects arose, the Cu LEIS areas are shown as a function of the Ce areas in Fig. 3 (c) with both He and Ne. As apparent from the figure, the Cu (He) area decreased linearly with the increase in Ce (He) area, implying the absence of neutralization matrix effects for the Ce/Cu(111) system when using helium. Consequently, the Ce (He) area and the decrease in the Cu (He) area are proportional to the number of cerium atoms in the topmost atomic layer, allowing quantitative evaluation of our data. From the slope of the Cu (He) *vs.* Ce (He) straight line the relative sensitivity factor for Ce was calculated to be S_{Ce}=0.0416. On the other hand, the Cu (Ne) *vs.* Ce (Ne) curve was clearly nonlinear, strongly suggesting a change in the Ne^+ neutralization probability either on Cu or on Ce as a function of cerium coverage. Here we suggest a simple way, how to discriminate between these two cases. In Fig. 3 (d) the Ce (Ne) area is shown as a function of the Ce (He) area. From Fig. 3 (c) it was deduced that the Ce (He) area is proportional to the fraction of the surface covered by Ce. For this reason, if an analogue proportionality holds for the Ce (Ne) area, then the Ce (Ne) *vs.* Ce (He) curve must be linear. However, a strong non-linearity can be observed in Fig. 3 (d), leading us to conclude that indeed a neutralization matrix effect exists for the Ce (Ne) signal. Consequently, the Ce (Ne) area is *not* proportional to the number of Ce atoms in the outermost atomic layer. On the other hand, the Cu (Ne) *vs.* Cu (He) curve is linear (inset of Fig. 3 (d), implying that the change in the Cu (Ne) signal is proportional to the fraction of the surface covered by Ce (Ne). Consequently, while the Cu (Ne) peak can be used for quantitative analysis of the Ce/Cu(111) system, it is not the case for the Ce (Ne) peak.

Once we determined our limits in the quantitative applicability of LEIS on Ce/Cu(111), we turn our attention to the growth of Ce on Cu(111). At small Ce coverages Ce (He), Cu (He) and Cu (Ne) areas all change linearly as a function of Ce dose, as shown by the linear fits in Fig. 3 (a) and (b). Remarkably, the extrapolation of the linear decrease of the Cu peaks crosses the abscissa at ~Θ_{Ce}=1 ML with both He and Ne. This observation has two implications: (i) the growth is two-dimensional (2D) at small coverages, up to Θ_{Ce}=0.5 ML; (ii) there is no significant diffusion of Ce into the subsurface of Cu(111) at room temperature in this coverage range.

Increasing the Ce coverage above 0.5 ML leads to a deviation from the linear behaviour of the Cu (He) and Cu (Ne) areas (Fig. 3 (a) and (b)). Consequently, Ce does not grow layer-by-layer on Cu(111). The observed non-linearity can be assigned either (i) to the onset of 3D growth already in this submonolayer coverage range (Stranski-Krastanov growth), or (ii) to an intermixing of Cu and Ce layers. The Cu (He) and Cu (Ne) peaks almost completely disappeared at Θ_{Ce}=2 ML (Fig. 2 and Fig. 3).

As it was mentioned in the Introduction, significant intermixing of Ce and Cu was found on a Cu film.[33] There are, however much less defects on our Cu(111) surface compared to a film, which may lead to stronger kinetic hindrance for inward diffusion of Ce. Note that after an initial 2D growth, the incorporation of Rh into the Ce overlayer was detected during the deposition of Ce on Rh(111) at room temperature.[35]

The interaction of O_2 and Ce on Cu(111)

In relation to the oxygen-cerium interaction on Cu(111), we first investigated the effect of O_2 adsorption on the Cu(111) surface partially covered by Ce at room temperature. The comparison of LEIS spectra collected before and after oxygen adsorption demonstrates that the interaction with oxygen enhances the 3D character (*i.e.* the average height) of Ce clusters on Cu(111): exposure to oxygen led to an increase in the Cu peak, while the presence of oxygen on cerium resulted in the diminution of the Ce peak (Fig. 4). Note that the O_2 exposure applied here (1 L) induced only a slight decrease (by 10%) in the Cu (He) peak, when oxygen was dosed on the pure Cu(111) (Fig.1).

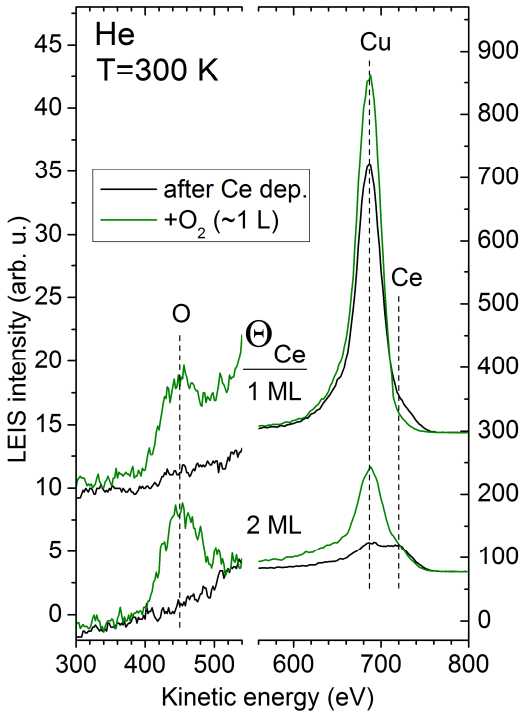

Fig. 4. LEIS spectra obtained with He after the deposition of Ce on Cu(111) at 300 K and after subsequent adsorption of O_2 (~1 L) at 300 K.

In the next experiment CeO_2 was deposited on Cu(111) evaporating Ce at a substrate temperature of 523 K in a background of O_2. A similar recipe was frequently applied in previous studies, yielding oriented CeO_2(111) films.[20,21] However, in our experiment a somewhat higher oxygen pressure was used (3×10^{-6} mbar instead of 5×10^{-7} mbar) in order to further improve the stoichiometry. LEIS peak areas obtained with He are shown in Fig. 5 (a) as a function of CeO_2 coverage.

Physical Chemistry Chemical Physics Accepted Manuscript

This journal is © The Royal Society of Chemistry 2012

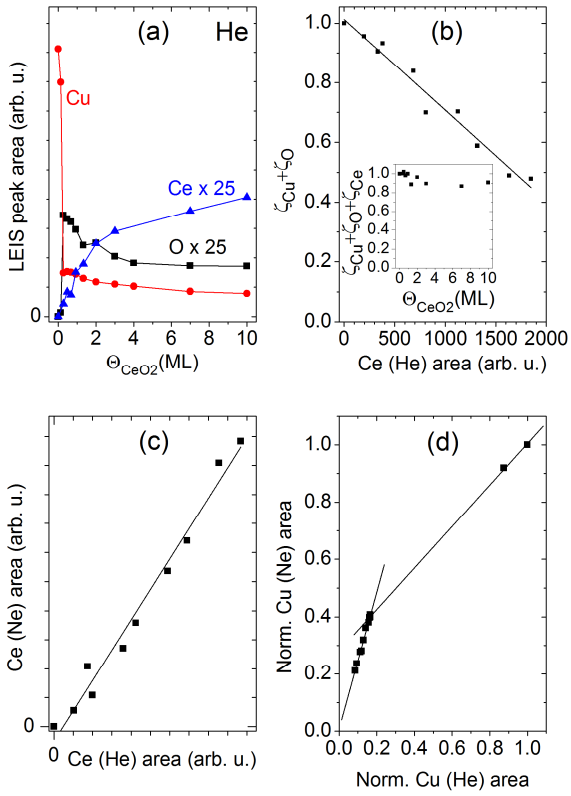

Fig. 5: Deposition of Ce on Cu(111) at T=523 K in an O_2 background of 3×10^{-6} mbar. (a): areas of LEIS peaks obtained with He as a function of CeO_2 coverage. (b): the fraction of the surface covered by Cu and O, calculated using the relative sensitivity factor S_O=0.0191, displayed as a function of the Ce (He) area. *Inset:* $\zeta_{Cu}+\zeta_O+\zeta_{Ce}$ as a function of CeO_2 coverage. (c): the Ce area obtained with neon as a function of Ce area obtained with helium. (d) the normalized Cu area obtained with neon as a function of the normalized Cu area obtained with helium. For (b), (c) and (d) linear fits are also presented.

At the initial phase of deposition, up to a CeO_2 coverage of ~0.3 ML, a very steep decrease in the Cu component, and an increase in the O peak was observed, while the Ce contribution was still rather small. In this coverage range the adsorption of oxygen on Cu(111) is the dominating process. At higher Ce doses both Cu and O areas decreased, in parallel with the gradual enhancement of the Ce area (Fig. 5 (a)), as the fraction of the surface covered by CeO_2(111) increased. In Fig. 5 (b) the fraction of the surface covered by Cu and O, calculated with the relative sensitivity factor obtained above for O (S_O) in the O_2 adsorption measurement, is shown as a function of the Ce (He) area. The linear behaviour indicates the absence of neutralization effects for the Cu-O-Ce ternary system, when using He. The applicability of the relative sensitivity factors S_O and S_{Ce} to the ternary system was checked controlling the fulfilment of the balance (inset of Fig. 5 (b)):

$$1 = \zeta_{Cu} + \zeta_O + \zeta_{Ce} = \frac{A_{Cu}+\frac{A_O}{S_O}+\frac{A_{Ce}}{S_{Ce}}}{A_{Cu}(0)} \qquad (3)$$

The agreement was reasonably good, within 10 %, in the whole CeO_2 coverage range investigated.

Interestingly, the neutralization matrix effect, observed for the Ce peak with neon during the deposition of metallic Ce did not arise when CeO_2 was grown on the copper surface. This is demonstrated by the linearity of the Ce (Ne) *vs.* Ce (He) curve presented in Fig. 5 (c), and very probably can be attributed to the changes in the valence of Ce. The normalized Cu (Ne) area displayed as a function of the normalized Cu (He) area can be well fitted with a broken line (Fig. 5 (d)). The slope (0.72) in the region of higher copper intensities agrees well with the slope (0.67) obtained for the Cu (Ne) *vs.* Cu (He) curve in the O_2 adsorption measurement (Fig. 1 (d)). This coincidence can be understood considering that in the initial phase of CeO_2 deposition the attenuation of the Cu intensities are mostly due to the adsorption of oxygen. At later stages of the growth further decrease in the Cu peaks are caused by the formation of 3D CeO_2 particles.

During our experiments about CeO_2(111) deposition, some variation was observed in the wetting of the Cu(111) surface by the ceria layer. This is in part reasonable, since the CeO_2(111)/Cu(111) system is thermodynamically of non-wetting nature, and slight changes in the experimental conditions can result in measurable differences in the film morphology. For this reason, in-situ monitoring of film continuity by LEIS proved to be very useful. The applied oxygen partial pressure had a well detectable impact on the tightness of the film. CeO_2(111) growth was monitored at two oxygen pressures: 5×10^{-7} mbar, and 3×10^{-6} mbar. Typical LEIS spectra obtained with He and Ne after the deposition of 16 ML of CeO_2 on Cu(111) are presented in Fig. 6.

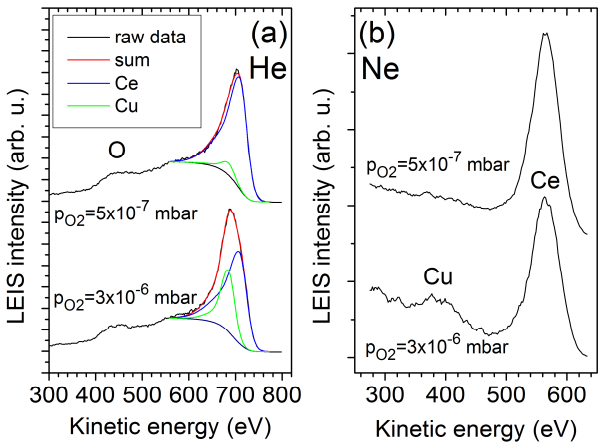

Fig. 6: LEIS spectra obtained with (a) He, and (b) Ne after the deposition of 16 ML of CeO_2 on Cu(111) at different O_2 pressures.

Apparently, while at the preparation pressure of 3×10^{-6} mbar a small Cu peak (~0.015 ML) was typically observed, the application of the lower pressure led to the almost complete disappearance of copper from the outermost atomic layer (~0.003 ML detected). The observed Ce (Ne)/Ce (He) area ratios agreed well with the slope of Fig. 5 (c).

Physical Chemistry Chemical Physics Accepted Manuscript

The better wetting achieved at the lower oxygen pressure, however, was accompanied by a slightly worse stoichiometry, as deduced from Ce 3d XPS spectra, shown in Fig. 7 (a). As known from literature, the Ce 3d peak shape of CeO_2 can be approximated with six peaks, due to shake-down processes involving the valence region, while the Ce 3d peak shape of Ce_2O_3 can be fitted with 4 peaks.[18,46,47] For a more detailed picture, which might allow a deeper understanding of the core levels and the properties of Ce in these spectra, we refer to.[48] While at $p_{O2}=3\times10^{-6}$ mbar 2 % of cerium ions were in the 3+ oxidation state, at $p_{O2}=5\times10^{-7}$ mbar this value increased to 4%. In accordance with previous results an asymmetry for the lowest binding energy doublet for CeO_2 was allowed in the fitting.[49,50] The reducing effect of the Ne^+ dose used for one LEIS spectrum was also checked by XPS. The observed change in the Ce 3d region was near to the limit of detection: the Ce^{3+}/Ce_{total} ratio increased by about 0.5-1%. A LEIS spectrum with Ne^+ was collected before each spectrum of Fig. 7 (a). The applied oxygen pressure had also a significant impact on the oxidation state of the uncovered copper surface/the copper ceria interface as well. It is well-known that the identification of various oxidation states of copper is much easier if the Cu LMM Auger region of the XPS spectrum is also considered,[51] as the shift of the Cu $2p_{3/2}$ peak is very small upon oxidation of metallic Cu to Cu_2O.

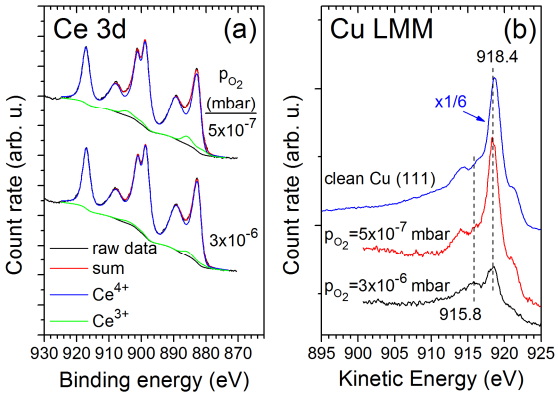

Fig. 7: The Ce 3d XPS region (a) and the Cu LMM Auger region (b) after the deposition of 16 ML of CeO_2 on Cu(111) at varying O_2 pressures. In (b) the Cu LMM region for the clean Cu(111) surface is also presented.

The Cu LMM region for the clean Cu(111) surface and for the 16 ML CeO_2/Cu(111) film obtained with different oxygen pressures is shown in Fig. 7 (b). At the lower pressure the peak shape was very similar to the metallic one, but at $p_{O2}=3\times10^{-6}$ mbar a relatively strong feature appeared at 915.8 eV, which is assigned to Cu^{1+}. We cannot exclude that at $p_{O2}=3\times10^{-6}$ mbar a part of copper ions are accumulated on top of the CeO_2 film, possibly in the form of a mixed oxide, since Ne^+ sputtering led to the disappearance of the Cu (He) and Cu (Ne) LEIS peaks and to the attenuation of Cu 2p and Cu LMM features in the XPS spectrum, accompanied by a more metallic character in the Cu LMM region (not shown). Since the recipe at $p_{O2}=5\times10^{-7}$ mbar is identical to the one applied in previous studies, where the oriented growth of CeO_2(111) on Cu(111) was demonstrated,[20,21] very probably the same (1.5×1.5) epitaxy holds also for our case.

Conclusions

The controlled growth of metallic Ce and CeO_2 was studied on Cu(111) by LEIS and XPS. A special attention was paid to the occurrence of neutralization effects, which would significantly hinder quantitative evaluation of LEIS data.

(i) No neutralization effects were identified related to the adsorption of O_2 on Cu(111).

(ii) As regards the interaction of metallic Ce and Cu(111), no neutralization effects were observed when using He^+, but it arose for the Ce peak collected with Ne^+. The initial growth mode of Ce is two dimensional up to Θ_{Ce}=0.5 ML, but nearly total coverage of the copper surface is achieved only at Θ_{Ce}=2 ML.

(iii) The CeO_2 overlayer was prepared evaporating Ce in an O_2 background. No neutralization effects were observed either with helium or neon. The growth mode is three dimensional. LEIS proved to be very efficient in checking the continuity of the ceria films, which was investigated at two different oxygen pressures.. At $p_{O2}=3\times10^{-6}$ mbar the film was not completely closed even at relatively large coverages (16 ML), and a significant part of copper atoms were oxidized to Cu^{1+}. Deposition of CeO_2 at $p_{O2}=5\times10^{-7}$ mbar was characterized by a nearly perfect wetting, with metallic copper atoms at the interface, but the stoichiometry of the ceria layer was slightly more reduced.

Acknowledgements

This work was supported by the Alexander von Humboldt Foundation within the Research Group Linkage Programme, by the Hungarian Scientific Research Fund (OTKA) through the K81660 project, and by COST Action CM1104.

Notes and references

[a] Department of Applied and Environmental Chemistry, University of Szeged, Rerrich Béla tér 1., Szeged, H-6720, Hungary
[b] MTA-SZTE Reaction Kinetics and Surface Chemistry Research Group, Rerrich Béla tér 1., Szeged, H-6720, Hungary
* corresponding author: ovari@chem.u-szeged.hu

1 *Catalysis by Ceria and Related Materials,* 2nd ed., Catalytic Science Series, Vol. 12, ed.: A. Trovarelli, P. Fornasiero, Imperial College Press, London, 2013, pp. 1-888.
2 J. Llorca, J. –A. Dalmon, P. R. de la Piscina, N. Homs, *Appl. Catal. A: General*, 2003, **243**, 261.
3 C. Sun, H. Li and L. Chen, *Energy Environ. Sci.*, 2012, **5**, 8475.
4 L. Óvári, S. Krick Calderon, Y. Lykhach, J. Libuda, A. Erdőhelyi, C. Papp, J. Kiss, H. -P. Steinrück, *J. Catal.*, 2013, **307**, 132.
5 Zs. Ferencz, A. Erdőhelyi, K. Baán, A. Oszkó, L. Óvári, Z. Kónya, C. Papp, H.-P. Steinrück, and J. Kiss, *ACS Catal.*, 2014, **4**, 1205.
6 G. A. Deluga, J. R. Salge, L. D. Schmidt, X. E. Verykios, *Science* 2004, **303**, 993.
7 S. D. Park, J. M. Vohs, R. J. Gorte, *Nature* 2000, **404**, 265.

This journal is © The Royal Society of Chemistry 2012

Physical Chemistry Chemical Physics Accepted Manuscript

8 H. –J Freund, *Surf. Sci.* 2002, **500**, 271.
9 U. Diebold, *Surf. Sci. Rep.*, 2003, **48**, 53.
10 Q. Fu, T. Wagner, *Surf. Sci. Rep.* 2007, **11**, 431.
11 L. Óvári, L. Bugyi, Z. Majzik, A. Berkó J. Kiss, *J. Phys. Chem. C* 2008, **112**, 18011.
12 L. Óvári, A. Berkó, N. Balázs, Z. Majzik, J. Kiss, *Langmuir* 2010, **26**, 2167.
13 A. Berkó, N. Balázs, G. Kassab, L. Óvári, *J. Catal.* 2012, **289**, 179.
14 D. R. Mullins, P. V. Radulovic, S. H. Overbury, *Surf. Sci.* 1999, **429**, 186.
15 J.-L. Lu, H.-J. Gao, S. Shaikhutdinov, H.-J. Freund, *Surf. Sci.* 2006, **600**, 5004.
16 A. Siokou, R. M. Nix, *J. Phys. Chem. B* 1999, **103**, 6984.
17 V. Matolín, J. Libra, I. Matolínová, V. Nehasil, L. Sedláček, F. Šutara, *Appl. Surf. Sci.* 2007, **254**, 153.
18 F. Šutara, M. Cabala, L. Sedláček, T. Skála, M. Škoda, V. Matolín, K. C. Prince, V. Cháb, *Thin Solid Films* 2008, **516**, 6120.
19 T. Staudt, Y. Lykhach, L. Hammer, M. A. Schneider, V. Matolín, J. Libuda, *Surf. Sci.* 2009, **603**, 3382.
20 F. Dvořák, O. Stetsovych, M. Steger, E. Cherradi, I. Matolínová, N. Tsud, M. Škoda, T. Skála, J. Mysliveček, and V. Matolín, *J. Phys. Chem. C* 2011, **115**, 7496.
21 V. Matolín, I. Matolínová, F. Dvořák, V. Johánek, J. Mysliveček, K. C. Prince, T. Skála, O. Stetsovych, N. Tsud, M. Václavů, B. Šmíd, *Catal. Today* 2012, **181**, 124.
22 R. Wrobel, Y. Suchorski, S. Becker, H. Weiss, Surf. Sci. 602 (2008) 436.
23 F. Yang, J. Graciani, J. Evans, P. Liu, J. Hrbek, J. F. Sanz, and J. A. Rodriguez, *J. Am. Chem. Soc.* 2011, **133**, 3444.
24 M. Alexandrou, R. M. Nix, *Surf. Sci.* 1994, **321**, 47.
25 F. H. P. M. Habraken, E. P. Kieffer, G. A. Bootsma, *Surf. Sci.* 1979, **83**, 45.
26 F. Solymosi, J. Kiss, *Surf. Sci.* 1981, **104**, 181.
27 F. Jensen, F. Besenbacher, E. Lægsgaard and I. Stensgaard, *Surf. Sci. Lett.* 1991, **259**, L774.
28 F. Jensen, F. Besenbacher and I. Stensgaard, *Surf. Sci.* 1992, **269/270**, 400.
29 T. Matsumoto, R. A. Bennett, P. Stone, T. Yamada, K. Domen, M. Bowker, *Surf. Sci.* 2001, **471**, 225.
30 A. Önsten, M. Göthelid, U. O. Karlsson, *Surf. Sci.* 2009, **603**, 257.
31 T. Ďuchoň, F. Dvořák, M. Aulická, V. Stetsovych, M. Vorokhta, D. Mazur, K. Veltruská, T. Skála, J. Mysliveček, I. Matolínová, and V. Matolín, *J. Phys. Chem. C* 2014, **118**, 357.
32 H. H. Brongersma, M. Draxler, M. de Ridder, P. Bauer, *Surf. Sci. Rep.* 2007, **62**, 63.
33 N. A. Braaten, J. K. Grepstad, and S. Raaen, *Phys. Rev. B* 1989, **40**, 7969.
34 P. R. Subramanian, D. E. Laughlin, *Bull. Alloy Phase Diag.*, 1988, **9**, 322.
35 E. Napetschnig, M. Schmid, P. Varga, *Surf. Sci.* 2004, **556**, 1.
36 D. A. Shirley, *Phys. Rev. B* 1972, **5**, 4709.
37 R. C. Weast, M. J. Astle (Eds.), CRC Handbook of Chemistry and Physics, 60th ed. CRC Press, Boca Raton, Florida, 1979–1980.
38 Y. Zhao, W. B. Holzapfel, *J. Alloys Comp.* 1997, **246**, 216.
39 P. Kürnsteiner, R. Steinberger, D. Primetzhofer, D. Goebl, T. Wagner, Z. Druckmüllerova, P. Zeppenfeld, P. Bauer, *Surf. Sci.* 2013, **609**, 167.
40 H. Niehus, *Surf. Sci.* 1983, **130**, 41.
41 D. J. Godfrey, D. P. Woodruff, *Surf. Sci.* 1981, **105**, 459.
42 D. J. Godfrey, D. P. Woodruff, *Surf. Sci.* 1981, **105**, 438.
43 E. Platzgummer, M. Borrell, C. Nagl, M. Schmid, P. Varga, *Surf. Sci.* 1998, **412/413**, 202.
44 M. P. Seah, W. A. Dench, *Surf. Interf. Anal.* 1979, **1**, 2.
45 J. H. Scofield, *J. Electr. Spectrosc. Relat. Phenom.* 1976, **8**, 129.
46 A. Fujimori, *Phys. Rev. B* 1983, **28**, 4489.
47 A. Pfau, K. D. Schierbaum, *Surf. Sci.* 1994, **321**, 71.
48 C. J. Nelin, P. S. Bagus, E. S. Ilton, S. A. Chambers, H. Kuhlenbeck, H.-J. Freund, *Int. J. Quantum Chem.* 2010, **110**, 2752.
49 T. Skála, F. Šutara, K. C. Prince, V. Matolín, *J. Electron Spectrosc. Relat. Phenom.* 2009, **169**, 20.
50 M. Engelhard, S. Azad, C. H. F. Peden, and S. Thevuthasan, *Surf. Sci. Spect.* 2004, **11**, 73.
51 J. P. Espinós, J. Morales, A. Barranco, A. Caballero, J. P. Holgado, and A. R. González-Elipe, *J. Phys. Chem. B* 2002**, 106**, 6921.

Physical Chemistry Chemical Physics Accepted Manuscript